

Nano-textured Pb (Zr_{0.52}Ti_{0.48})O₃/ZnO hetero-structure on silicon substrate

Govind N. Sharma^{1,2}, Shankar Dutta¹, Ratnamala Chatterjee², Sushil Kumar Singh^{1*}

¹Solid State Physics Laboratory, DRDO, Lucknow Road, Timarpur, Delhi 110054, India

²Department of Physics, Indian Institute of Technology, Hauz Khas, New Delhi 110016, India

*Corresponding author. Tel: (+91) 1123903433; E-mail: singhksushil@gmail.com; sk.singh@sspl.drdo.in

Received: 07 March 2016, Revised: 25 April 2016 and Accepted: 22 June 2016

ABSTRACT

Metal oxide based hetero-structures (like Pb (Zr_xTi_{1-x}) O₃ – ZnO) can be used for wide variety of future sensors and electronic devices. This paper presents growth and electrical properties of nano-textured (110) Pb (Zr_{0.52}Ti_{0.48}) O₃/ (001) ZnO heterostructure on oxidized silicon substrate by RF sputtering technique. The grain sizes of ZnO and PZT films are found to be around 30 nm and 80 nm respectively. Resistivity of the ZnO layer is found to be $1 \times 10^9 \Omega\text{-cm}$. The electrical properties of the film are studied by creating in-plane electrodes on top of the PZT/ZnO heterostructure film. The remnant polarization of the film is found $\sim 47 \mu\text{C}/\text{cm}^2$ at 200 kV/cm. Dielectric constant of the film is found to be 300 at 1 kHz. The film also showed a low leakage current density of $\sim 10^{-5} \text{ A}/\text{cm}^2$ at 200 kV/cm applied electric field. The nano-textured (110) Pb (Zr_{0.52}Ti_{0.48}) O₃/ (100) ZnO heterostructure integrated with inter-digital-transducers and microelectronic is well suitable for low-cost, robust, programmable passive micro sensors for military structure and systems such as aircraft, missiles. Copyright © 2016 VBRI Press.

Keywords: PZT; ZnO; hetero-structure; ferroelectric.

Introduction

Metal-oxide thin films, like ZrO₂, HfO₂, TiO₂, CeO₂, BiFeO₃, Pb (ZrTi) O₃ (PZT), ZnO etc., have received significant devotion in wide variety of applications [1-9]. They are exclusively used in thin film capacitor, metal-oxide-semiconductor (MOS) transistor [2-3], ferroelectric [5], multiferroic [7-8], and other diverse areas. In recent years, metal-oxides are being integrated with micro-electromechanical system (MEMS) for many novel applications [9-11].

Out of the many metal-oxide thin films, PZT (Pb (Zr_xTi_{1-x}) O₃) is being widely studied for its excellent ferroelectric and piezoelectric properties [5, 9-10, 12-23]. The application of PZT is ranging from nonvolatile memories to MEMS based energy harvester [9-10]. Several reports have been published on growth of PZT thin films (of different Zr: Ti ratios) and their optical and electrical properties. Hundreds of research articles are published on PZT thin films but majority of them is polycrystalline in nature. However, for reliable electronic and photonic applications, control of the crystallographic orientation (preferably epitaxial) PZT thin films on semiconducting substrates is very important to get improved ferroelectric properties with minimal fatigue. For MEMS applications, epitaxial or preferentially orientated PZT layers can be more useful due to their enhanced ferroelectric and strong strain-polarization coupling.

Properties of metal-oxide thin films are known to be highly reliant on their crystalline quality and orientations which are primarily determined by the choice of substrate/buffer layer and deposition technique. Many

attempts are being also made to integrate epitaxial quality PZT films directly on silicon. However, the integration of epitaxial PZT layers onto silicon wafers remains a huge challenge mainly due to the stability and interfaces of PZT with silicon. Thus a buffer layers is being introduced between PZT thin film and silicon substrate to make a stable interface. Yin et al. [10] reported about epitaxial growth and the electrical characteristics of single crystalline PZT thin film on SrTiO₃ buffered Si (001) substrate by sol-gel technique. Isarakorna et al. [9] discussed about silicon membrane actuated by an epitaxial PZT thin film on SrTiO₃ buffer layer for localized-mass sensing applications. Shi et al. [14] presented (001) oriented morphotropic PZT film (85 nm) grown epitaxially on [001]-oriented SrTiO₃-buffered (6 nm) Si-wafer. Harigai et al. [15] reported about the piezoelectric behavior of (001) oriented PZT film ($\sim 3 \mu\text{m}$ thick) on Ir coated Si wafers by sputtering technique. Sol-gel deposited (110) oriented PZT films (2 μm thick) on strontium titanate bottom layer and their ferroelectric and piezoelectric properties are discussed by Ambika et al. [16].

Sambri et al. [17] investigated structural and electrical properties of epitaxial PZT thin films grown on SrTiO₃ buffered (001) silicon wafers by sputtering technique. Borowiak et al. [18] discussed about epitaxial growth and electrical properties of PZT thin films deposited by pulsed laser deposition (PLD) on SrTiO₃ buffered Si (001). Hao et al. [19] represented enhanced ferroelectric properties of epitaxial PZT film with LaAlO₃ buffer on SrRuO₃/ LaAlO₃ (SRO/LAO) substrates using PLD. Wakiya et al. [20] investigated the nucleation and growth behavior of epitaxial PZT thin films (MOCVD grown) on cleaved MgO (100)

substrates by x-ray photoelectron spectroscopy. Dekkers *et al.* [21] presented crystalline PZT thin films between metallic-oxide SrRuO₃ electrodes prepared using PLD on CeO₂/ yttria-stabilized zirconia buffered silicon (001) substrates. Moon *et al.* [22] discussed the characteristics of ferroelectric PZT films epitaxially grown on CeO₂ (111)/ Si (111) substrates. Recently, highly controlled (001) and (110) oriented PZT films on Si-substrate were achieved using Ca₂Nb₃O₁₀ and Ti_{0.87}O₂ nano-sheet buffer layers respectively [23].

We found that majority of the previously published literature discussed about epitaxial PZT layer on SrTiO₃ buffer layer [9-10, 14, 16]. Few reports are also discussed about epitaxial PZT layer on other buffer layers (Ir, MgO, CeO₂, ZrO₂, SrRuO₃, LaAlO₃ etc.). Like SrTiO₃, ZnO is also very promising material for electronic and photonic applications. It has good transparency, high electron mobility, wide bandgap (direct, 3.3 eV), and strong room-temperature luminescence [13]. Smooth ZnO thin films with uniform microstructure showed a good insulating characteristic [24-28]. It is also reported that PZT/ZnO based Metal-Ferroelectric-Insulator-Semiconductor (MFIS) is suitable for FET based non-volatile ferroelectric memory [28]. Interface quality of ferroelectric/semiconductors hetero-structure is of most importance for effective coupling and ZnO offers the chemically stable structure with PZT [29]. Integrating ferroelectric oxide with semiconductor allow us to utilized the functional behavior such as Ferro/ Pyro/ Piezo-electric of the films for advance multifunctional devices.

Like many other metal-oxide thin films, the electrical as well as optical properties of PZT-ZnO hetero-structure greatly rely on their thickness as well as crystalline quality (epitaxial or textured or polycrystalline). The modification in electronic structures due to joining two dissimilar crystals (PZT: Tetragonal and ZnO: hexagonal) is also impart changes in electrical properties of the hetero-structure. There are few reports on polycrystalline PZT layer on ZnO buffered silicon [4, 13, 28] but yet not any attempt is made to integrate epitaxial/ oriented ZnO and PZT layers on oxidized silicon surface. Integrating of PZT films at low temperature with high degree of crystal orientation to the Si-wafer and in-plane sensing has practical applications in piezoelectric based MEMS devices. Moreover, both PZT and ZnO are large band gap materials so they also have the potential for future optoelectronic devices.

In this paper, hetero-structure of (110)-oriented Pb(Zr_{0.52}Ti_{0.48}) O₃ layer and (001)-oriented ZnO layer is deposited on oxidized silicon substrate by RF sputtering technique. Microstructure of the ZnO and textured PZT films were studied. Two adjacent electrodes were used to measure the in-plane electrical properties of the PZT/ZnO heterostructure thin film. The aim of this work is to demonstrated that in-plane electrical properties can be measured in nano-textured (110) Pb (Zr_{0.52}Ti_{0.48}) O₃/ (100) ZnO heterostructure fabricated on Si substrates. It is easy to integrated with inter-digital-transducers and microelectronic using the MEMS fabrication technology resulting low-cost, robust, programmable passive micro sensors, which has applications in military structure and systems such as aircraft, missiles.

Experimental

The PZT/ZnO heterostructure is deposited on the oxidized silicon surface. The silicon surface is oxidized by placing the sample in a three-zone horizontal furnace heated at 1150°C in oxygen (flow rate: 2L/min) environment for 90 minutes. Prior to the oxidation process, the silicon substrate is cleaned by standard Radio Corporation of America (RCA) cleaning procedure (first developed by RCA Laboratory in 1970). In this process, the wafer is cleaned in two solutions - first in NH₄OH, H₂O₂, and deionized water (DI) mixture and then in HCl, H₂O₂, and DI water mixture. This helps in reducing the contaminations present on the wafer surface. The native oxide generated during the RCA cleaning is then removed in diluted (1%) hydrofluoric acid. Then, the sample is thoroughly cleaned in DI water, dried, and subsequently loaded in sputtering chamber for the deposition. To grow high quality epitaxial PZT thin films on oxidized silicon surface, proper intermediate layer is required. In this work, ZnO is used as buffer layer to grow high quality oriented PZT layer on 50 mm diameter Si (001) wafers by RF sputtering technique. Prior to the depositions, ZnO and Pb (Zr_{0.52}Ti_{0.48}) O₃ targets are pre-sputtered in an argon atmosphere in order to remove contaminated surface oxides on the targets. The ZnO film is deposited (deposition rate: 1 Å/ s) at a constant RF power of 60 W with 10 mtorr pressure. For the deposition, substrate temperature is fixed at 400°C distance with target to substrate kept at 5 cm. Thereafter, the PZT layer is deposited (deposition rate: 1 Å/ s) at 75 W RF power with 15 mtorr pressure. In this case, the substrate temperature is fixed at 600°C with target to substrate distance kept at 3.5 cm.

The phase and crystalline structure of the PZT/ZnO heterostructure thin film is analyzed using grazing incidence XRD in thin film geometry using Cu K α radiation (Model: PANalytical XPert Pro MRD HRXRD system). Surface morphologies and cross-section of the films are observed by Field-Emission Scanning Electron Microscopy (FE-SEM) (SUPRA-50). The ferroelectric hysteresis (P-E) loop for the PZT/ ZnO heterostructure thin film is measured using PE Loop Tracer (Precision Premier II, Radiant Technologies, USA). The leakage current of the sample is measured using with Keithley Parameter Analyzer (4200-SCS).

Results and discussion

The x-ray diffraction analysis results of the ZnO and PZT thin films are presented in Fig. 1. The XRD pattern of the ZnO film indicates single phase highly oriented along (002) ZnO films on oxidized silicon wafer as shown in Fig. 1(a). No other peaks are observed except the sharp peak around 69 ° which is due to the Si (004) peak coming from (001) oriented silicon substrate. Previously published reports support that, the ZnO films on silicon are predominantly (002) oriented at lower oxygen pressure (<15 m torr) during sputtering [7, 30-34]. The ZnO film orientation starts changing with the increasing oxygen pressure [7-8, 24, 31, 34]. Both the XRD peaks corresponding peaks of ZnO and substrate are found to be very intense, therefore no hump in the lower angle XRD data are observed (corresponding to amorphous SiO₂ layer). The XRD pattern

in **Fig. 1(b)** shows growth of the (110) oriented PZT film on top of the ZnO film. Thus simultaneously shows (002) peak of ZnO thin film and (004) peak of the silicon substrate. The small peak appearing around 64° in Fig 1(b) is due to the PZT (220) plane. This confirms the highly texture nature of the PZT film on ZnO layer. The PZT films grown on (002) oriented ZnO film are either (111) oriented or (110) oriented [8, 24]. If the PZT film deposited around $650 - 700^\circ\text{C}$, it is found to be (111) oriented [8, 24]; whereas, it is found to be (110) oriented when deposited below 650°C [8]. **Fig. 1(c)** shows schematic atomic arrangements of PZT (blue empty circle) and ZnO (red solid circle), where the dotted rectangles represent (110) surface unit cells of PZT and red hexagons represent the c-oriented ZnO unit cells. The lattice mis-match along the [110] direction of PZT is $\sim 0.97\%$. However, along the [001] direction of PZT, no simple epitaxial relationship is found between the lattices, but a commensurate relationship of $3c\text{ PZT} \cong 4a\text{ ZnO}$ is found to give a lattice mismatch of 5.2% along the [001] PZT direction. Using the XRD data and Scherrer equation, average crystallite sizes of the ZnO and PZT films are estimated. The crystallite sizes of ZnO and PZT films are found to be around 30 nm and 70 nm respectively.

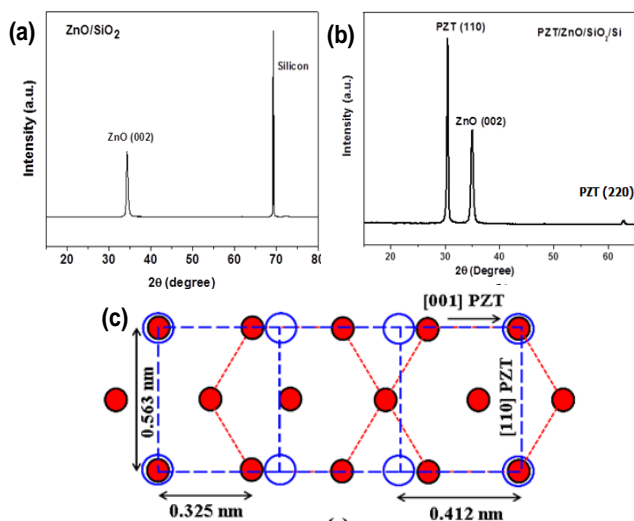


Fig. 1. X-ray diffraction pattern of (a) ZnO film (b) PZT/ ZnO heterostructure on silicon substrate. (c) Schematic of possible in-plane epitaxial orientation relationship between (110) PZT and (002) ZnO. The red circles denote the lattice points of ZnO and hollow blue circle represent the PZT lattice points.

Surface morphologies and cross-sections of the ZnO thin films are observed by the scanning electron micrograph (SEM) as shown in **Fig. 2** (a) and (b) respectively. **Fig. 2** (a) shows the surface morphology of the film indicates grain sizes approximately 30 nm which matches well with the crystallite size estimated from XRD data. Cross-section of the ZnO film shows columnar structure, which were aligned on the substrate with the c-axis orientation perpendicular to the substrate surface as shown in Fig. 2(b). From **Fig. 2(b)**, thickness of the ZnO thin film is found to be 200 nm . The minimization of the surface energy during the growth plays the crucial role and controlled the surface morphology which results columnar structure of (002) orientation is achieved.

Fig. 3 (a) and (b) depict the surface morphologies and cross-sections of the PZT thin film deposited on ZnO/SiO₂/Si surface respectively.

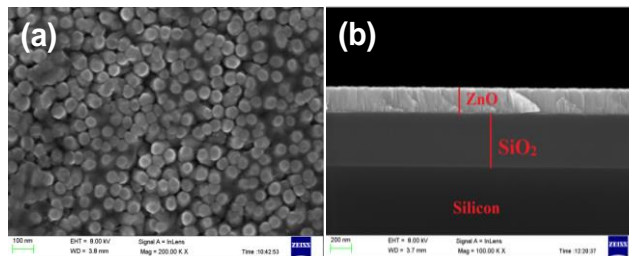


Fig. 2. SEM image of ZnO thin films on silicon substrate: (a) surface morphology (b) cross section.

The grains of PZT thin film are very well controlled and achieved smooth surface in large area as shown in **Fig. 3** (a). The average grain size of PZT films is approximately 80 nm which is quite close to the crystallite size estimated from XRD data. From **Fig. 3(b)**, thickness of the PZT layer is estimated to be $\sim 300\text{ nm}$. From the cross-section image, interface between the PZT and ZnO heterostructure is found to be quite sharp. Thus from the micrographs and XRD data it may be deduced that the (001) oriented columnar ZnO film acts as seed layer for the growth of (110) orientation columnar PZT film on amorphous SiO₂ layer.

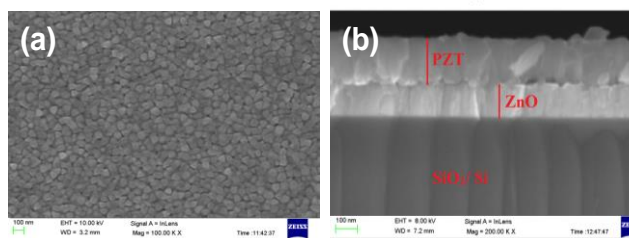


Fig. 3. SEM image of PZT/ZnO heterostructure thin film on silicon substrate: (a) surface morphology (b) cross section.

Dielectric properties of the (110) oriented PZT thin film is measured as a function of frequency ($1\text{ kHz} - 1\text{ MHz}$) at room temperature as shown in **Fig. 4**. At 1 kHz , the film exhibited a dielectric constant value of 300 . The value of dielectric constant values found to be decreased slightly (from 300 to 280) with an increase in the applied frequency; thus the PZT thin film exhibit an excellent dielectric constant at higher frequency. Dielectric loss ($\tan \delta$) of the sample is found to decrease with the increase in frequency. The reason for decrease of both dielectric constant and dielectric loss may be due to inability of the electric dipoles to be in pace with frequency of applied electric field at high frequency. Maxwell-Wagner polarization and space charge polarization are seems to be responsible for high values of $\tan \delta$ at low frequencies. The dielectric permittivity is better than that reported by Isarakorn et al. ($70-100$) [9]. Ambika et al. [16] has reported superior dielectric permittivity of 1545 and dielectric loss ~ 0.04 with moderate remnant polarization. Hao et al. [19] and Dekkers et al. [21] have not reported the dielectric permittivity of the PZT films deposited by them.

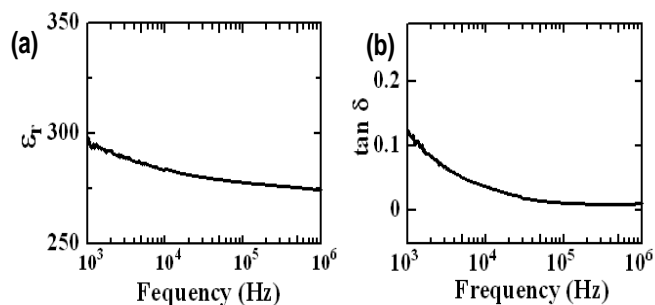


Fig. 4. Dielectric properties of PZT/ ZnO heterostructure thin film on silicon substrate.

Fig. 5 shows the leakage current density of (110) oriented PZT thin film as a function of applied voltage. The thin film exhibits low in-plane leakage current density (10^{-5} A/ cm^2) at 200 kV/ cm applied electric field. Like the ferroelectric study, there is no reported literature on in-plane leakage current of textured/ epitaxial PZT thin film. Amibika *et al.* [16] reported out of plane leakage current density of 2.8×10^{-7} A/ cm^2 at $E=100$ kV/ cm. Sambri *et al.* [17] presented a leakage current density of $20 \mu\text{A}/ \text{cm}^2$ at 5 V. Borowiak *et al.* [18] couldn't measure the leakage current density. Hao *et al.* [19] reported out of plane leakage currents (no current density values) in PZT/ SRO and PZT/ LAO/ SRO films to be 2.6×10^{-4} A and 4.1×10^{-6} A at 15 V, respectively. Dekker *et al.* [21] reported a leakage current $\sim 10^{-5}$ A at 100 kV/ cm. Moon *et al.* [22] reported the leakage current density in PZT thin film to be 2.08×10^{-7} A/ cm^2 measured at 5 V without mentioning remnant polarization.

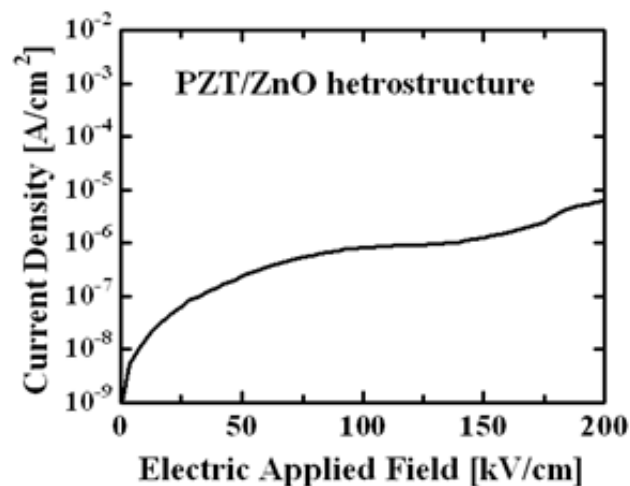


Fig. 5. Leakage current density of PZT/ZnO heterostructure thin film on silicon substrate.

Generally, ferroelectric thin films are deposited platinized silicon substrates [4-6, 9, 13, 15-16, 19] and their electrical properties are measured across its thickness by applying bias between top and bottom electrodes. However, for realization of variety of ferroelectric based smart MEMS devices, integration of ferroelectric thin films on non-platinum coated silicon wafers are equally important. But, there are very little reports on the deposition/ integration of ferroelectric thin films on non-platinum coated silicon substrates [29, 35-36]. The PZT/ ZnO

heterostructure film is deposited on SiO_2/Si , there is no bottom electrode. Therefore, the electrical properties of the heterostructure thin film are studied in-plane via creating $200 \mu\text{m}$ diameter electrodes on top of the film.

The Electric field induced polarization measurements have been performed at 100 Hz frequency at room temperature as shown in **Fig. 6**. The PZT/ ZnO heterostructure film exhibits remnant polarization (P_r) of $24 \mu\text{C}/ \text{cm}^2$ at 80 kV/ cm applied electric field. In-plane ferroelectric P-E loop measurement requires higher applied electric field in comparison to the measurement with bottom layer. This is due to gap between the adjacent electrodes. Here, resistivity of the ZnO layer is very important. Low resistivity of ZnO layer will give a leakage current path during the in-plane electrical measurements. So, in a separate experiment, resistivity of the ZnO layer (without depositing PZT layer on top of it) is measured by Van-der Pauw method. Resistivity of the ZnO layer is found to be $1 \times 10^9 \Omega\text{-cm}$. Generally, ZnO is a wide band-gap semiconductor material with resistivity $\sim 10^1\text{-}10^6 \Omega\text{-cm}$ [7, 33]. Jeong *et al.* [7], Raimondi *et al.* [30], Carcia *et al.* [31], Fortunato *et al.* [32], and Lee *et al.* [33] have shown that higher resistivity (up-to $10^{13} \Omega\text{-cm}$) of ZnO thin film can be achieved by sputtering technique. The reason for the relatively high resistivity of the ZnO layer seems to be due to the oxygen vacancy in the ZnO thin film [7, 30, 34].

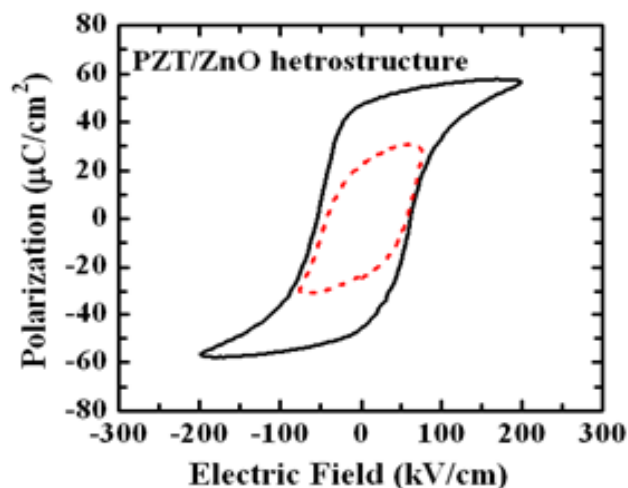


Fig. 6. P-E hysteresis loop of PZT/ZnO heterostructure thin film on silicon substrate.

At 80 kV/ cm applied electric field, the hysteresis loops of the PZT/ ZnO heterostructure is found to be unsaturated in nature. It seems to be due to the insufficient electric field as well as restricted domain wall movement. It is well known that the presence of defects, like grain boundaries, voids etc. are responsible for this constraint of ferroelectric domain wall movements [37-38]. **Fig. 3** already showed that the multilayer has grain size of 80 nm; thus there is large number of grains boundaries between two adjacent electrodes. We believe that presence of these large number of grain boundaries is accountable for restriction of the domain wall movements in the film.

It may also be due to interface effect between ZnO and PZT layers as shown in **Fig. 3 (b)**. To overcome this restriction and to get saturated P-E loop, large electric

potential need to be applied [39]. When we applied electric field 120 kV/cm, the saturated P-E loop is observed. The PZT/ZnO heterostructure film exhibits remnant polarization (P_r) of 47 $\mu\text{C}/\text{cm}^2$ with applied electric field 200 kV/cm. We didn't find any reports discussed about in-plane ferroelectric properties of textured/epitaxial PZT thin film. A few number of previously published literature discussed about in-plane electrical properties of polycrystalline ferroelectric thin films [9-10, 35-36]. The present study showed improved remnant polarization compared to the out of plane remnant polarization reported by Chen *et al.* (15 $\mu\text{C}/\text{cm}^2$) [12], Wang *et al.* (28 $\mu\text{C}/\text{cm}^2$) [13], Ambika *et al.* (12.5 $\mu\text{C}/\text{cm}^2$) [16] and Dekkers *et al.* (20 $\mu\text{C}/\text{cm}^2$) [21]. However, our value is inferior to the out of plane remnant polarizations reported by Isarakorn *et al.* (70 $\mu\text{C}/\text{cm}^2$) [9], Sambri *et al.* (70 $\mu\text{C}/\text{cm}^2$) [17] and Hao *et al.* (58 $\mu\text{C}/\text{cm}^2$) [19].

It is advantageous to detect the electrical contribution of the ferroelectric thin film in-plane via fabricating interdigitated terminal (IDT) structures on top of the film. This structure provides the additional freedom in designing and machining of MEMS based device fabrication. Schematic representation of in-plane electrical measurement of ferroelectric thin films (a) IDT structure (b) electric field lines distribution shown in the Fig. 7. The electric field lines tend to prefer ferroelectric medium compared to the air/surface leakage between the consecutive IDT fingers as presented in Fig 7(b).

The quantum of electric field lines will depend on the permittivity of the medium. Thus, PZT layer should have maximum field lines compared to the ZnO and SiO₂ layers. Due to the presence of large number of electrodes in IDT structure, the electric field lines is expected to be neither homogeneous in magnitude nor in direction [35]. However, if the IDT finger gap (w) is larger compared to the thickness (t) of the film, the vertical component of the electric field in the film beneath the electrode fingers contribute much less than the horizontal component of the electric displacement between two fingers. Thus, the electric field lines between the adjacent electrode fingers are assumed to be homogeneous and parallel to the film's plane, whereas the electric lines beneath the electrodes is neglected and the potential in these regions can be assumed to be uniform. Therefore, under these assumptions, the IDT will form a number of parallel plate capacitors connected in parallel with PZT as a dielectric medium.

The present study is very important in finding in-plane electrical properties of ferroelectric materials. In-plane ferroelectric measurement by creating inter-digitated terminals (IDT) is being used in sensing and transducing application in many MEMS as well as surface acoustic wave (SAW) based devices [40]. The present PZT/ZnO heterostructure thin film along with IDT structures can be utilized for different MEMS and SAW based devices. Moreover, the textured/epitaxial nature of the large band gap PZT/ZnO heterostructure can also be used in many photonics devices. The optical band gap of the ZnO and PZT-ZnO hetero-structure are found to be 3.3eV and 3.23eV respectively. Detail of the optical measurement data for the band gap is communicated separately. The optical band gap of ZnO layer is found to be good agreement with the previously published results [13]. From previously

published literatures, it is well known that optical band gap of PZT layers can be direct (~ 4.05 eV) as well as indirect (3.10-3.20 eV) [41]. The shifts in optical band gap of the PZT-ZnO hetero-structure seems to be due to the combined effect strain between PZT and ZnO layers as well as indirect bandgap component of PZT.

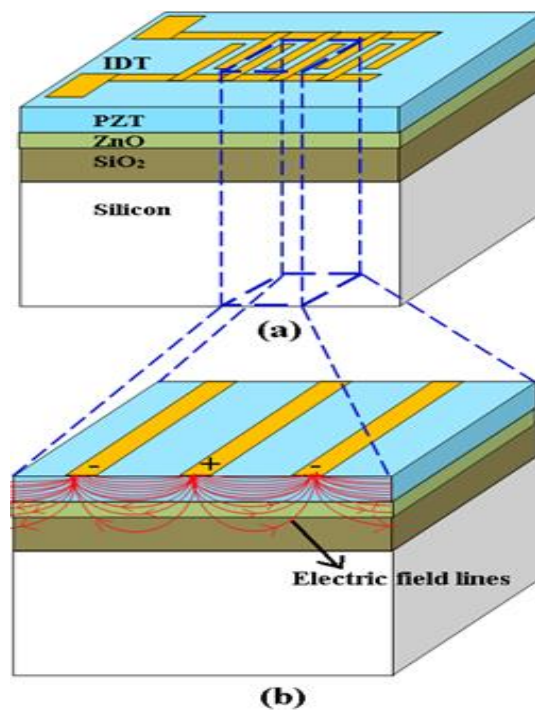


Fig. 7. Schematic representation of in-plane electrical measurement of ferroelectric material: (a) IDT structure (b) electric field lines distribution.

Conclusion

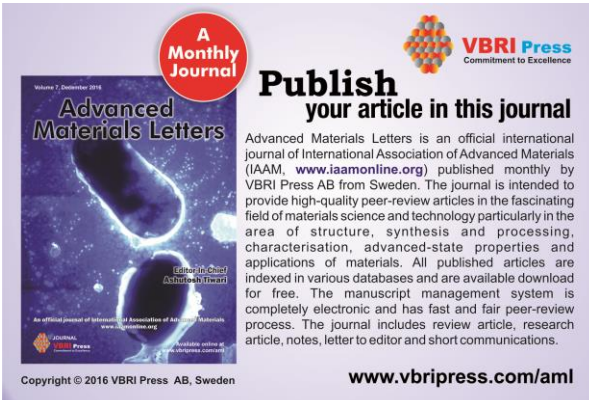
Metal oxide based hetero-structures can be applied for wide variety applications for future sensors and electronic devices. Out of many metal oxides, PZT and ZnO have excellent electrical and optical properties. In this work, growth and electrical properties of nano-textured PZT-ZnO hetero-structure on SiO₂/Si surface by sputtering technique is discussed. Prior to the deposition of high quality PZT thin film on amorphous (SiO₂) surface, a (001) oriented ZnO buffer/seed layer is introduced. X-ray diffraction showed phase pure perovskite structure with (110) oriented PZT film. SEM micrograph of the film indicate the grain sizes of ZnO and PZT films are found to be ~ 30 nm and ~ 80 nm respectively. In-plane electrical characteristics of the film are studied. The film exhibited a remnant polarization of ~ 47 $\mu\text{C}/\text{cm}^2$ at 200 kV/cm applied electric field. Dielectric constant of the film is found to be 300 measured at 1 kHz. A leakage current density of 10^{-5} A/cm² is observed at 200 kV/cm applied electric field. Nano-textured PZT/ZnO heterostructure along with IDT structure provides the addition freedom in designing and machining of MEMS based devices.

Acknowledgements

This project was funded by SSPL, DRDO (Task-24). The author wishes to acknowledge Prof. Davander Kaur, Physics Department, IIT, Roorkee for using their thin film deposition facility and useful discussion. The authors also acknowledge Director, SSPL for his continuous support.

Reference

- Henrich V.E.; Cox P. A.; The Surface Science of Metal Oxides, Cambridge University Press, UK, 1994.
DOI: [10.1002/aic.690440230](https://doi.org/10.1002/aic.690440230)
- He G.; Fang Q.; Zhang J. X.; Zhu L. Q.; Liu M.; Zhang L. D.; *Nanotechnology*, **2005**, *16*, 1641.
DOI: [10.1088/0957-4484/16/9/040](https://doi.org/10.1088/0957-4484/16/9/040)
- Dutta S.; Leeladhar; Pandey A.; Thakur O.P.; Pal R.; *J. Vac. Sci. Tech. A*, **2015**, *33*, 021507.
DOI: [10.1116/1.4904978](https://doi.org/10.1116/1.4904978)
- Dutta S.; Pandey A.; Yadav I.; Thakur O. P.; Laishram R.; Pal R.; Chatterjee R.; *J. Appl. Phys.*, **2012**, *112*, 084101.
DOI: [10.1063/1.4759123](https://doi.org/10.1063/1.4759123)
- Singh S. K.; Kim Y.K.; Funakubo H.; Ishiwaru H.; *Appl. Phys. Lett.*, **2006**, *88*, 162904.
DOI: [10.1063/1.2196477](https://doi.org/10.1063/1.2196477)
- Singh S.K.; *Thin Solid Films*, **2013**, *527*, 126.
DOI: [10.1016/j.tsf.2012.11.062](https://doi.org/10.1016/j.tsf.2012.11.062)
- Jeong W.J.; Kim S.K.; Park G.C.; *Thin Solid Films*, **2006**, *180*, 506.
DOI: [10.1016/j.tsf.2005.08.213](https://doi.org/10.1016/j.tsf.2005.08.213)
- Shukla, S. K., Tiwari, A., Parashar, G. K., Mishra, A.P., Dubey, G.C., *Talanta*, **2009**, *80* (2), 565-571.
DOI: [10.1016/j.talanta.2009.07.026](https://doi.org/10.1016/j.talanta.2009.07.026)
- Isarakorna D.; Brianda D.; Sambrib A.; Garigliob S.; Triscone J.M.; Guyc F.; Reinerd J.W.; Ahnd C.H.; de-Rooija N.F.; *Sens. Act. B*, **2011**, *153*, 54.
DOI: [10.1016/j.snb.2010.10.009](https://doi.org/10.1016/j.snb.2010.10.009)
- Yin S.; Niu G.; Vilquin B.; Gautier B.; Le Rhun G.; Defay E.; Robach Y.; *Thin Solid Films*, **2012**, *520*, 4572.
DOI: [10.1016/j.tsf.2011.11.073](https://doi.org/10.1016/j.tsf.2011.11.073)
- Sharma U.; Dutta S.; *J. Mater. Sci.: Mater. Electron.*, **2014**, *25*, 5546.
DOI: [10.1007/s10854-014-2342-z](https://doi.org/10.1007/s10854-014-2342-z)
- Chen D.Y.; Murphy T.E.; Phillips J.D.; *Thin Solid Films*, **2005**, *491*, 301.
DOI: [10.1016/j.tsf.2005.06.007](https://doi.org/10.1016/j.tsf.2005.06.007)
- Wang X.S.; Wang Y.J.; Yin J.; Liu Z.G.; *Scripta Mater*, **2002**, *46*, 783.
DOI: [10.1016/S1359-6462\(02\)00076-3](https://doi.org/10.1016/S1359-6462(02)00076-3)
- Shi Y.; Cuff M.; Niu G.; Le Rhun G.; Vilquin B.; Saint Girons G.; Bachelet R.; Gautier B.; Robach Y.; Gemeiner P.; Guiblin N.; Defay E.; Dkhil B.; *J. Appl. Phys.*, **2014**, *115*, 214108.
DOI: [10.1063/1.4881818](https://doi.org/10.1063/1.4881818)
- Harigai T.; Adachi H.; Fujii E.; *J. Appl. Phys.*, **2010**, *107*, 096101.
DOI: [10.1063/1.3406253](https://doi.org/10.1063/1.3406253)
- Ambika D.; Kumar V.; Imai H.; Kanno I.; *Appl. Phys. Lett.*, **2010**, *96*, 031909.
DOI: [10.1063/1.3293446](https://doi.org/10.1063/1.3293446)
- Sambri A.; Gariglio S.; Pardo A.T.; Triscone J.M.; Stéphan O.; Reiner J. W.; Ahn C. H.; *Appl. Phys. Lett.*, **2011**, *98*, 012903.
DOI: [10.1063/1.3532110](https://doi.org/10.1063/1.3532110)
- Borowiak A.S.; Niu G.; Pillard V.; Agnus G.; Lecoeur Ph.; Albertini D.; Baboux N.; Gautier B.; Vilquin B.; *Thin Solid Films*, **2012**, *520*, 4604.
DOI: [10.1016/j.tsf.2011.10.139](https://doi.org/10.1016/j.tsf.2011.10.139)
- Hao L.; Zhu J.; Zeng H.; Zhang Y.; Zhang W.; Li Y.; *Thin Solid Films*, **2011**, *520*, 784.
DOI: [10.1016/j.tsf.2011.01.409](https://doi.org/10.1016/j.tsf.2011.01.409)
- Wakiya N.; Kuroyanagi K.; Xuan Y.; Shinozaki K.; Mizutani N.; *Thin Solid Films*, **2000**, *372*, 156.
DOI: [10.1016/S0040-6090\(00\)01013-0](https://doi.org/10.1016/S0040-6090(00)01013-0)
- Dekkers M.; Nguyen M.D.; Steenwelle R.; teRiele P.M.; Blank D.H.A.; Rijnders G.; *Appl. Phys. Lett.*, **2009**, *95*, 012902.
DOI: [10.1063/1.3163057](https://doi.org/10.1063/1.3163057)
- Moon B.K.; Ishiwaru H.; Tokumitsu E.; Yoshimoto M.; *Thin Solid Films*, **2001**, *385*, 307.
DOI: [10.1016/S0040-6090\(00\)01900-3](https://doi.org/10.1016/S0040-6090(00)01900-3)
- Chopra A.; Bayraktar M.; Bijkerk F.; Rijnders G.; *Thin Solid Films*, **2015**, *589*, 13.
DOI: [10.1016/j.tsf.2015.04.039](https://doi.org/10.1016/j.tsf.2015.04.039)
- Meng X.; Yang C.; Fu W.; Wan J.; *Mater. Lett.*, **2012**, *83*, 179.
DOI: [10.1016/j.matlet.2012.06.015](https://doi.org/10.1016/j.matlet.2012.06.015)
- Meng X.; Yang C.; Chen Q.; Yang J.; *J. Mater. Sci.: Mater. Electron.*, **2013**, *24*, 160.
DOI: [10.1007/s10854-012-1004-2](https://doi.org/10.1007/s10854-012-1004-2)
- Pintilie I.; Pasuk I.; Ibanescu G. A.; Negrea R.; Chirila C.; Vasile E.; Pintilie L.; *J. Appl. Phys.*, **2012**, *112*, 104103.
DOI: [10.1063/1.4765723](https://doi.org/10.1063/1.4765723)
- Kumar A.; Mishra S. K.; *Adv. Mat. Lett.*, **2014**, *5*, 479
DOI: [10.5185/amlett.2014.564](https://doi.org/10.5185/amlett.2014.564)
- Cagin E.; Chen D.Y.; Siddiqui J.J.; Phillips J. D.; *J. Phys. D: Appl. Phys.*, **2007**, *40*, 2430.
DOI: [10.1088/0022-3727/40/8/003](https://doi.org/10.1088/0022-3727/40/8/003)
- Murali P.; Maeder T.; Sagalowicz L.; Hiboux S.; Scales S.; Naumovic D.; Agostino R.G.; Xanthopoulos N.; Mathieu H.J.; Patthey L.; Bullock E.L.; *J. Appl. Phys.*, **1998**, *83*, 3835.
DOI: [10.1063/1.366614](https://doi.org/10.1063/1.366614)
- Raimondi D.L.; Kay E.; *J. Vac. Sci. Tech.*, **1970**, *7*, 96.
DOI: [10.1116/1.1315841](https://doi.org/10.1116/1.1315841)
- Carcia P.F.; McLean R.S.; Reilly M.H.; Nunes G.; *Appl. Phys. Lett.*, **2003**, *82*, 1117.
DOI: [10.1063/1.1553997](https://doi.org/10.1063/1.1553997)
- Fortunto E.M.C.; Barquinha P.M.C.; Piementel A.C.M.B.G.; Goncalves A.M.F.; Marques A.J.S.; Pereira L.M.N.; Martins R.F.P.; *Adv. Mater.*, **2005**, *17*, 590.
DOI: [10.1002/adma.200400368](https://doi.org/10.1002/adma.200400368)
- Lee J.B.; Park C.K.; Park J.S.; *J. Korean Phys. Soc.*, **2007**, *50*, 1073.
DOI: [10.3938/jkps.50.1073](https://doi.org/10.3938/jkps.50.1073)
- Kim W.; Choi M.; Yong K.; *Sens. Act. B*, **2015**, *209*, 989.
DOI: [10.1016/j.snb.2014.12.072](https://doi.org/10.1016/j.snb.2014.12.072)
- Zhang Q.Q.; Gross S.J.; Tadigadapa S.; Jackson T.N.; Djuth F.T.; Trolier-McKinstry S.; *Sens. Act. A*, **2003**, *105*, 91.
DOI: [10.1016/S0924-4247\(03\)00068-2](https://doi.org/10.1016/S0924-4247(03)00068-2)
- Kumar A.; Scott J.F.; Martinez R.; Srinivasan G.; Katiyar R.S.; *physica status solidi (a)*, **2012**, *209*, 1207.
DOI: [10.1002/pssa.201228154](https://doi.org/10.1002/pssa.201228154)
- Shu W.; Wang J.; Zhang T.Y.; *J. Appl. Phys.*, **2012**, *112*, 064108.
DOI: [10.1063/1.4752269](https://doi.org/10.1063/1.4752269)
- Choudhury S.; Li Y.L.; Krill C.; Chen L.Q.; *Acta Mater.*, **2007**, *55*, 1415.
DOI: [10.1016/j.actamat.2006.09.048](https://doi.org/10.1016/j.actamat.2006.09.048)
- Tsang C. H.; Wong C. K.; Shin F. G.; *J. Appl. Phys.*, **2005**, *98*, 084103.
DOI: [10.1063/1.2103417](https://doi.org/10.1063/1.2103417)
- Varadan V.K.; Vinoy K.J.; Gopalakrishna S.; Smart Material Systems and MEMS: Design and Development Methodologies, John Wiley and Sons, USA, 2006.
DOI: [10.1002/0470093633.fmatter](https://doi.org/10.1002/0470093633.fmatter)
- Izyumskaya N.; Alivov Y.L.; Cho S.J.; Morko H.; Lee H.; Kang Y.S.; *Critical Rev. Solid State Mater. Sci.*, **2007**, *32*, 111.
DOI: [10.1080/10408430701707347](https://doi.org/10.1080/10408430701707347)



A Monthly Journal

Publish your article in this journal

Advanced Materials Letters is an official international journal of International Association of Advanced Materials (IAAM, www.iaamonline.org) published monthly by VBRI Press AB from Sweden. The journal is intended to provide high-quality peer-review articles in the fascinating field of materials science and technology particularly in the area of structure, synthesis and processing, characterisation, advanced-state properties and applications of materials. All published articles are indexed in various databases and are available download for free. The manuscript management system is completely electronic and has fast and fair peer-review process. The journal includes review article, research article, notes, letter to editor and short communications.

Copyright © 2016 VBRI Press AB, Sweden

www.vbripress.com/aml